Available online at www.elixirpublishers.com (Elixir International Journal)

Corrosion

Elixir Corrosion 65 (2013) 20122-20128

ISSN: 2229-712X

Quantum chemical studies and corrosion inhibition efficiency for 1,2,3-Benzotriazol on carbon steel alloy in 1M hydrochloric acid

M.Abd-El-Raouf* and E.A. Khamis
Egyptian Petroleum Research Institute

ARTICLE INFO

Article history:
Received: 9 November 2013;
Received in revised form:
10 December 2013;
Accepted: 23 December 2013;

Keywords
Carbon steel,
SEM,
Inhibition,
Adsorption.

ABSTRACT

The 1,2,3-Benzotriazol were evaluated in the present work as corrosion inhibitors for protection of the carbon steel in chloride solutions. The corrosion protection performance was investigated by means of weight loss and DC polarization and electrochemical impedance spectroscopy (EIS). Scanning electron microscope was used to study the surface topography during corrosion tests. The results show that all inhibitors under study confer corrosion protection to the carbon steel forming a thin organic layer on the substrate surface. The following quantum chemical indices such as the charge density distribution, highest occupied molecular orbital (HOMO), the lowest unoccupied molecular orbital (LUMO), energy gap, ΔN and dipole moment (u) were considered. The inhibition efficiencies obtained from the employed methods are nearly closed. From the obtained data it was found that, the inhibition efficiency increases with increasing the inhibitor concentration until the optimum one.

Introduction

Acidic solutions are extensively used in industry for industrial-equipment cleaning, oil-wells acidization, and pretreatment of compositions **[1–3]**. Hydrochloric acid is widely used in pickling solutions. In corrosion inhibitors, it is necessary to reduce the dissolution of metals in these acidic environments.

The efficiency of inhibition depends on the corrosion environment, metallic material, and the type and molecular structure of the inhibitor **[4–7].** Various organic inhibitors were studied as corrosion inhibitors and it was reported that these compounds are effective inhibitors **[8–12]**. The inhibition efficiency of organic inhibitors is due to their adherent absorption to the metal surface **[13, 14].** These compounds form protective films on the metal surface and protect metals against the pitting attack. The organic compounds containing heteroatoms, such as P, S, N, and O, which have lone pairs of electrons and can donate these, are useful inhibitors for metals **[14–16].**

The aim of the present work is to study the corrosion inhibition of carbon steel in hydrochloric acid with and without additions of different amounts of inhibitor. The inhibition performance was evaluated by weight loss, potentiodynamic polarization, electrochemical impedance spectroscopy (EIS) and scanning electronic microscopy(SEM).

Experiments

Solutions

The aggressive solution, 1 M HCl, was prepared by dilution of analytical grade 37% HCl with distilled water. The concentration range of the prepared inhibitors was from 100 to 600 ppm used for corrosion measurements. All solutions were prepared using distilled water.

Weight loss measurements

The steel sheets of 7.0 ×2.0× 0.3 cm dimensions were abraded with different grades of emery papers, washed with distilled water, degreased with acetone, dried and kept in a desiccator. After weighing accurately by a digital balance with high sensitivity the specimens were immersed in solution containing 1 M HCl solution with and without various concentrations of the investigated inhibitors. After 4 h exposure, the specimens were taken out rinsed thoroughly with bi-distilled water, dried and weighted accurately again. Three parallel experiments were performed for each test. The average weight loss ,Δ*W*(mg)was calculated using the following equation**[17]**:

$$\Delta W = W_1 - W_2 \qquad (1)$$

where W_1 and W_2 are the average weight of specimens before and after exposure, respectively.

Preparation of working electrodes

The working carbon steel electrode specimens were cut from a cylindrical rod to a length of 5 cm and covered by Teflon leaving only 0.5 cm^2 of the surface area exposed to solution. The electrical conductivity was provided by a copper wire **[18]**. The chemical composition of working electrode (wt, %) was: 0.07% C, 0.24% Si, 1.35% Mn, 0.017% P, 0.005% S, 0.16% Cr, 0.18% Ni, 0.12% Mo, 0.01% Cu and the remainder Fe. Before measurements, the surface of working electrode was mechanically abraded using different grades of emery papers, which ended with the 1000 grade. The disc was cleaned by washing with bi-distilled water, thoroughly degreased with acetone, washed once more with bi-distilled water and finally dried with a filter paper. For each test, a newly abraded electrode was used.

Weight Loss Measurements

Weight loss is the most common method to evaluate corrosion inhibition .Besides, it does not require sophisticated equipments for determination. The effectiveness of this compound as corrosion inhibitors for carbon steel in 1M HCl solutions has been investigated at different concentrations and The weight loss of carbon steel coupons after immersion in 1M HCl without or with different concentrations of using inhibitor were determined using following equations:

$$\Delta W = W1 - W2 \qquad (2)$$

Where: W1 and W2 are the weight of specimens before and after reaction, respectively

Tele:
E-mail addresses: abdelraouf1979@yahoo.com

and inhibition efficiency was determined by the equation

$$\eta\ \% = \frac{\Delta W - \Delta Wi}{\Delta W} x100 \qquad (3)$$

Where, Δ W and Δ Wi are the weight loss per unit area in absence and presence of additive, respectively. Through studying the effect of inhibition efficiency, the rate of corrosion (C.R) was calculated by the following equation:

$$\text{C.R} = \frac{W \times 3.45 \times 10^6}{A \times t \times D} \qquad (4)$$

Where: W is mass loss in gram, A is area in cm2, t is time in hours, D is density in g/cm3.

Experimental results of the weight loss versus time are graphically represented in Fig 1. From the plot, it's obvious that, the different concentrations (viz.100, 200,300,400 and 500) of the added inhibitor effectively decrease the weight loss compared to blank samples. Also, this inhibition increases with increasing the inhibitor concentration from 100to 500 ppm at 298 K. This may be due to accumulation of inhibitor molecules on the surface of the metal to form a complete monolayer adsorption. Also, the weight loss increases logically with increasing the time of immersion.

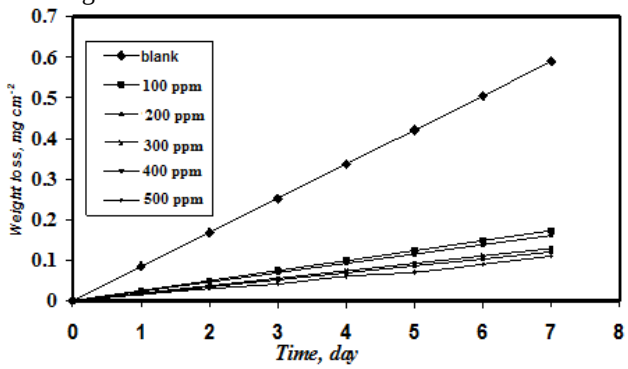

Fig 1: weight loss- time curves for carbon steel dissolution in 1 M HCl in absence and presence of inhibitor at different concentration (ppm) at 298 K.

Electrochemical measurements

The electrochemical measurements were carried out using Volta lab 40 (Tacussel-Radiometer PGZ301) potentiostate and controlled by Tacussel corrosion analysis software model (Voltamaster 4) at under static condition. The corrosion cell used had three electrodes. The reference electrode was a saturated calomel electrode (SCE). A platinum electrode was used as auxiliary electrode. The working electrode was carbon steel pipelines. All potentials given in this study were referred to this reference electrode. The working electrode was immersed in test solution for 30 minutes to a establish steady state open circuit potential (E_{ocp}). After measuring the E_{ocp}, the electrochemical measurements were performed. The polarization curves were obtained in the potential range from -250 to +250 mV(SCE) with 1 mV s^1 scan rate. EIS measurements were carried out in a frequency range of 100 kHz to 50 mHz with a 4 mV sine wave as the excitation signal at open circuit potential.

Surface morphology studies

The surface morphology of the steel specimens was examined after exposure to 1 M HCl in absence and presence of a certain concentration of the selected inhibitor (ET-40). JEOL 5410 scanning electron microscope SEM (Japan) was used for this investigation.

Quantum chemical study

All required molecular parameters was carried out based on MINDO3 semi-empirical method ever used for organic inhibitor's calculation **[19]** at a Unrestricted Hartree Fock (UHF) level which are implemented in Hyperchem 8.0. The molecules 2D sketch was obtained by ISIS Draw 2.1.4.

Results and discussion

Weight loss measurements

The corrosion rate (A) of steel specimens after 4 h exposure to1 M HCl solution with and without the addition of various concentrations of the investigated inhibitors was calculated and the obtained data are listed in **Table 1**. The corrosion rate, A (mg cm^{-2} h^{-1}), surface coverage (θ) and inhibition efficiency η_w of each concentration were calculated using the following equations **[19]**:

$$A = \frac{\Delta W}{St} \qquad (5)$$

$$\eta_w = \left(\frac{A_{uninh} - A_{inh}}{A_{uninh}}\right) \times 100 \qquad (3)$$

$$\theta = \frac{A_{uninh} - A_{inh}}{A_{uninh}} \qquad (6)$$

where ΔW is the average weight loss (mg), S is the surface area of specimens (cm^2), and t is the immersion time (h), A_{uninh} and A_{inh} are corrosion rates in the absence and presence of inhibitor, respectively. It is clear that η_w increased with increasing inhibitor concentration, while corrosion rate decreased. This could be due to the inhibitor molecules act by adsorption on the metal surface**[21]**.

The corrosion rate of carbon steel decrease when the concentration of compounds increases and inhibition efficiency attains its maximum value of 83.3% at 500 ppm. The inhibition efficiency obtained from weight loss measurements is lower than that from electrochemical experiments, this phenomenon attributed to weight loss experiments gives average corrosion rates, whereas the electrochemical experiments gives instantaneous corrosion rates.

Adsorption isotherm and standard adsorption free energy

Corrosion inhibition by organic compounds is mainly due to their ability to adsorb onto a metal surface to form a protective film. The adsorption of organic inhibitors at the metal/solution interface takes place through the replacement of water molecules by organic inhibitor molecules according to following process **[22]**.

$$Org_{(sol)} + xH_2O_{(ads)} \rightarrow Org_{(ads)} + xH_2O_{(sol)} \qquad (7)$$

where $Org_{(sol)}$ and $Org_{(ads)}$ are organic molecules in the solution and adsorbed on the metal surface, respectively, x is the number of water molecules replaced by the organic molecules. It is essential to know the mode of adsorption and the adsorption isotherm that can give valuable information on the interaction of inhibitor and metal surface**[23]**. Values of surface coverage (θ) corresponding to different concentrations of inhibitor, which calculated using the weight loss results at 303 K after 4 hours of immersion were used to determine which isotherm best described the adsorption process. The results obtained for the investigated inhibitors in 1 M HCl solution were tested with several adsorption isotherms. However, the best agreement was obtained using the Langmuir adsorption isothermal equation as follows**[24]:**

$$\frac{C_i}{\theta} = \frac{1}{K_{ads}} + C_i \qquad (8)$$

where C_i is the concentration of inhibitor and K_{ads} the adsorptive equilibrium constant. Langmuir's isotherm assumes that there is no interaction between the adsorbed molecules, the energy of adsorption is independent on the θ, the solid surface contains a fixed number of adsorption sites, and each site holds one adsorbed species. Plots of C_i / θ against C_i yield straight lines as shown in **Fig.2**, and the linear regression parameters are listed in **Table 3**. Both linear correlation coefficient (r) and slope are very close to 1, indicating the adsorption of the investigated inhibitors on steel surface obeys the Langmuir adsorption isotherm in 1 M HCl solution. The adsorptive equilibrium constant (K_{ads}) can be calculated from reciprocal of intercept of C_i/θ-C_i curve. K_{ads} is related to the standard free energy of adsorption ($\Delta G°_{ads}$) as shown the following equation **[25]**:

$$K_{ads} = \frac{1}{55.5} \exp\left(\frac{-\Delta G°_{ads}}{RT}\right) \quad (9)$$

where R is the gas constant (8.314 J mol^{-1} K^{-1}), T the absolute temperature (K), and the value 55.5 is the concentration of water in solution expressed in molar. The $\Delta G°_{ads}$ value is also listed in **Table 3**. The high values of K_{ads} and negative values of $\Delta G°_{ads}$ suggested that, surfactant molecules strongly adsorb on the steel surface. Generally, values of $\Delta G°_{ads}$ up to –20 kJ mol^{-1} are consistent with the electrostatic interaction between the charged molecules and the charged metal (physical adsorption), while those more negative than –40 kJ mol^{-1} involve sharing or transfer of electrons from the inhibitor molecules to the metal surface to form a coordinate type of bond (chemisorption) **[26]**. The values of $\Delta G°_{ads}$ for compound being less than (-40 kJ mol^{-1}) indicate physical adsorption, in addition to electrostatic interaction there may be some other interactions**[27].**

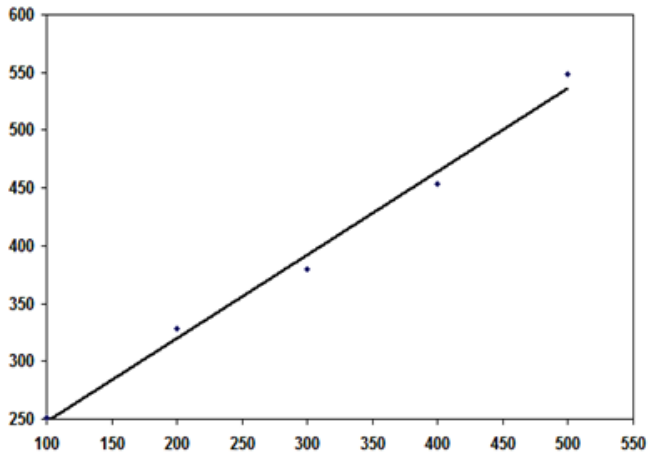

Figure 2: Langmiur adsorption plots of steel in 1 M HCl solution containing the investigated inhibitors at 303 K

Potentiodynamic polarization measurements

Fig. 3 shows polarization curves for carbon steel in 1M HCl with and without various concentrations of inhibitor. Values of associated electrochemical parameters such as corrosion potential (E_{corr}), corrosion current density (i_{corr}) , anodic and cathodic Tafel slopes (βa, βc)and the calculated η_p (%) are presented in **Table 4**. In this case, the inhibition efficiency is defined as follows:

$$\eta_p = \left(\frac{i_{corr(uninh)} - i_{corr(inh)}}{i_{corr(uninh)}}\right) \times 100 \quad (10)$$

where I^o_{corr} and I_{corr} are the corrosion current density of carbon steel without and with inhibitors in hydrochloric acid solutions. values of βc changed with increasing inhibitor concentration, which indicates the influence of the compounds on the kinetics of hydrogen evolution. The shift in the anodic Tafel slope βa may be due to the chloride ions /or inhibitor modules adsorb onto steel surface **[28].**

For anodic polarization curves of carbon steel with 500 ppm of inhibitor studied, it seems that the working electrode potential is higher than -300 mV/SCE, the presence of the inhibitor does not change the current versus potential characteristics, this potential can be defined as desorption potential **[29]**. The phenomenon may be due to the obvious metal dissolution, leading to a desorption of the triazole molecule from the electrode surface, in this case the desorption rate of the inhibitors is higher than its adsorption rate, so the corrosion current increases more obviously with rising potential **[30]**. As it can be seen from these polarisation results, the i_{corr} values decrease considerably in the presence of inhibitor and decreased with increasing inhibitor concentration, and we notice that the inhibition efficiency increased with inhibitor concentration reaching a maximum value of 85.8% at 500 ppm.

Table.4 shows that the inhibition efficiency increases with increasing the concentration of triazole compounds. They act as corrosion inhibitors suppressing both anodic and cathodic reaction by adsorbed on the carbon steel surface blocking the active sites **[31]**, and there is no definite trend in the shift of E_{corr} values, it can be recognized as a classification evidence of the compounds is mixed-type inhibitors **[32]**. The results obtained from the polarization technique in acidic solution were in good agreement with those obtained from the weight loss method.

The Electrochemical Impedance Spectroscopy (EIS)

Nyquist plots of triazole compounds in 1 M HCl solutions in the absence and presence of various concentrations of inhibitor. are given in **Fig.4**. The impedance spectra show that a single semicircle and the diameter of semicircle increases with increasing inhibitor concentration. These diagrams exhibit that the impedance spectra consist of one capacitive loop at high frequency, the high frequency capacitive loop was attributed to charge transfer of the corrosion process **[33].**

Various parameters such as charge-transfer resistance (*Rct*), double layer capacitance (*Cdl*) were obtained from impedance measurements and are shown in **Table 5.** *Rct* values were calculated from the difference in impedance at lower and higher frequencies as suggested by Tsuru et al. **[34].** *Cdl* values were calculated from the frequency at which the imaginary component of impedance was maximum (Zim max) using the reaction:

$$C_{dl} = \frac{1}{2\pi f_{max}} \times \frac{1}{R_{ct}} \quad (11)$$

where *f*max is the frequency at which the imaginary component of impedance is maximum. The inhibition efficiency got from the charge-transfer resistance is calculated by the following relation:

$$IE_{(R)}\% = \frac{R_{ct} - R^o_{ct}}{R_{ct}} \times 100 \quad (12)$$

where *Rct* and $R^o ct$ represent the resistance of charge transfer in the presence and absence of inhibitor, respectively. *Rct* is the diameter of the loop. the *Rct* values of all investigated triazole derivatives increase with increasing inhibitor concentration. At the same time the *Cdl* has opposite trend at the whole concentration range. These observations clearly bring out

the fact that the corrosion of carbon steel in 1M HCl is controlled by a charge transfer process. the decrease in *Cdl* is due to the gradual replacement of water molecules by the adsorption of the organic molecules at metal/solution interface, leading to a protective film on the steel surface, then decreasing the extent of dissolution reaction **[35].**

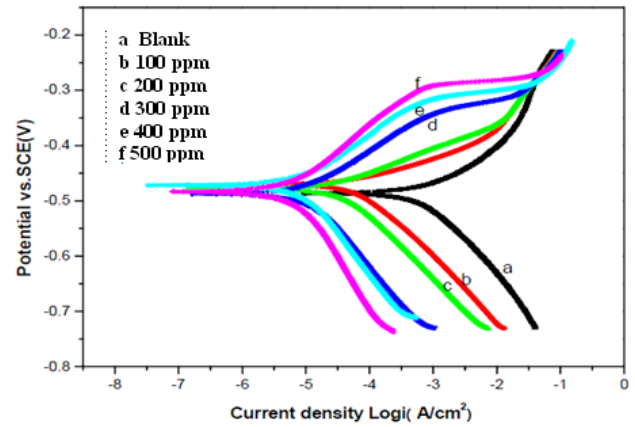

Figure 3: Polarization curves of carbon steel in 1M HCl containing various concentrations of inhibitor at 303K

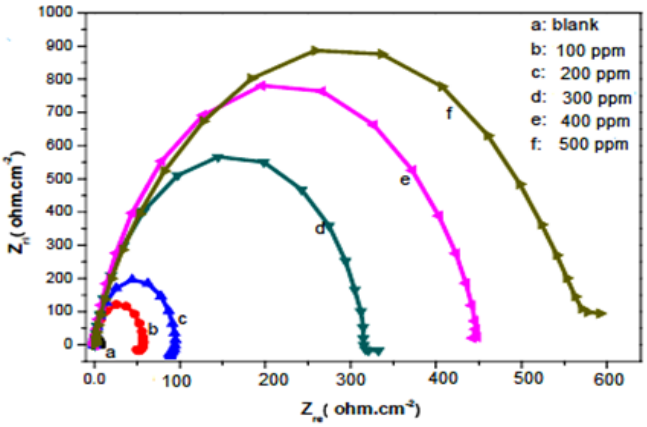

Figure 4: Nyquist diagrams for carbon steel in 1M HCl containing different concentrations of inhibitors at 303K

SEM analyses

SEM photographs obtained from mild steel surface after specimens immersion in 1M HCl solutions for 3 h in the absence and presence of 500ppm of inhibitor is shown in **Fig.5.** It can be observed from **Fig.5(a)** that the specimen surface was strongly damaged in the absence of the inhibitor. SEM images of the carbon steel surface after immersion in 1M HCl with 500ppm of inhibitor, are shown in **Fig.5(b)** , it can be seen that in presence of the inhibitor, the rate of corrosion is suppressed, it revealed that there is a good protective film adsorbed on specimens surface, which is responsible for the inhibition of corrosion.

Quantum chemical studies

Quantum chemical calculations have been widely used to study reaction mechanisms **[36].** They have also been proved to be a very powerful tool for studying inhibition of the corrosion of metals. It has been found that the effectiveness of a corrosion inhibitor can be related to its electronic and spatial molecular structure. In this study, the relationship between quantum chemical parameters and inhibition efficiency was investigated.

Some quantum chemical parameters, which are thought important to directly influence on electronic interaction between iron surface and inhibitor, are listed in **Table 6** namely the energy of the highest occupied molecular orbital (EHOMO), energy of the lowest unoccupied molecular orbital (ELUMO), the energy gap (ΔE), diploe moment (μ), the number of transferred electrons (ΔN), and the optimized geometry structures of the compounds were in **Figure 6**.

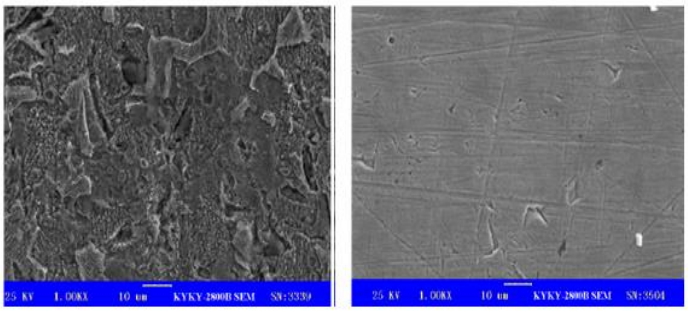

Fig.5 SEM micrographs of carbon steel samples at 303K, (a) after immersion in 1M HCl without inhibitor, (b) after immersion in 1M HCl in presence of 500ppm of inhibitor

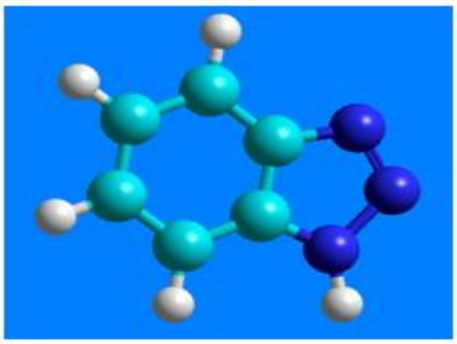

Fig 6: Equilibrium structure of the inhibitor

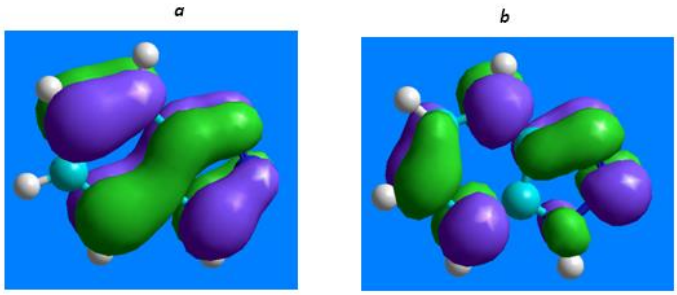

Fig 7: The frontier molecule orbital density distributions of Inhibitor (a) HOMO and (b) LUMO

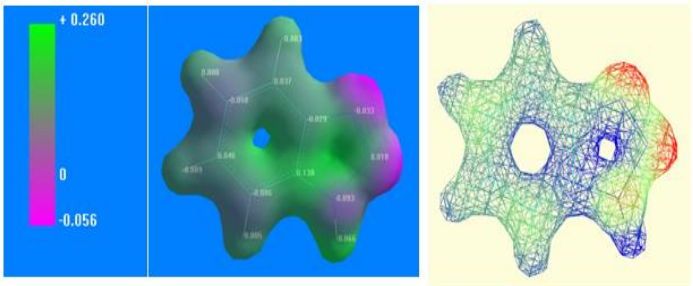

Fig 8: Molecular electrostatic potential map of the compound

According to the frontier molecular orbital theory, the formation of a transition state is due to an interaction between frontier orbitals (HOMO and LUMO) of reacting species **[37]**. Thus, the treatment of the frontier molecular orbitals separately from the other orbitals is based on the general principles governing the nature of chemical reactions. It has been proved that the higher the HOMO energy (EHOMO) level of the inhibitor is, the greater is the ease of offering electrons to the unoccupied d orbital of metallic iron and the greater is the inhibition efficiency of the inhibitor for iron **[38-44].** As can be seen from this **Table 6**, reveal that this inhibitor has high HOMO and low LUMO with high energy gap.

Table 1 : Corrosion Rate Dependence of Carbon Steel, the Degree of Surface Coverage (θ) at Different Concentrations of I_1 ZE_{20} in 1M HCl Solution at 298 K.

Concentration (ppm)	Rate of Corrosion (mpy)	(θ)
Blank	48.0	-
50	17.0	0.658
100	13.18	0.727
150	11.1	0.768
200	8.1	0.831
250	8.0	0.833

Table 2 :Corrosion parameters of steel after 4 h immersion in 1M HCl solution with and without various concentrations of inhibitors at 303 K.

Inhibitor	Concentration (ppm)	A(mg cm-2 hr-1)	θ	ηw (%)
Blank	0	0.473	---	---
Inhibitor	100	0.284	0.399	39.9
	200	0.184	0.610	61.0
	300	0.097	0.790	79.0
	400	0.056	0.882	88.2
	500	0.038	0.912	91.2

Table 3: Adsorption equilibrium constant (Kads) and standard free energy of adsorption (ΔG°) of the investigated surfactants for steel in 1 M HCl solution at 303 K

Inhibitor	Linear correlation coefficient (r)	Slope	Kads (104M–1)	-ΔG°ads (kJ mol–1)
SD1	0.990	0.890	5.72	-37.09

Table 4: Potentiodynamic electrochemical parameters for the corrosion of steel in 1 M HCl solution in the absence and presence different conc. of the investigated inhibitors at 303 K

Inhibitor	−Ecorr mV(SCE)	icorr (mA cm−2)	βa (mV dec−1)	-βc (mV dec−1)	ηp (%)
Blank	486	0.3695	131.1	-139.8	---
100	470	0.124	253.5	-173.0	0.66
200	478	0.1102	182.8	-151.2	0.70
300	486	0.1014	191.1	-165.9	0.72
400	471	0.0712	207.5	-158.1	0.80
500	483	0.0524	173.9	-141.0	0.85

Table 5 : Impedance electrochemical parameters derived from the Nyquist plots for steel in 1M HCl solution in the absence and presence different conc. of the investigated inhibitors at 303K.

Inhibitor	Rct (ohm.cm²)	Cdl (µF/cm²)	ηi(%)
Blank	117.5	121	---
100	337.0	42.26	0.69
200	274.3	25.31	0.70
300	292.3	22.76	0.71
400	335.2	16.42	0.82
500	299.0	12.99	0.84

Table 6: Quantum Chemical Parameters of the Investigated Inhibitor

Inhibitor	EHOMO(eV)	ELUMO(eV)	ΔE(eV)	µ(debye)	ΔN(eV)
I	-7.89	0.71-		1,76	

If an inhibitor does not only offer electrons to the unoccupied d orbital of metallic iron but can also accept the electrons in the d-orbital of metallic iron by using their antibonding orbital to form a feedback bond, then it may be considered as an excellent inhibitor. It has been proved that the lower the LUMO energy (ELUMO) level is, the easier is the acceptance of electrons of the d orbital of metallic iron **[38-44].**

Another point to be considered is the HOMO–LUMO gap (ΔE), i.e., the difference between the HOMO and LUMO energies for the compounds.

This is an important stability index and the concept of HOMO–LUMO energy gap is used to develop theoretical models which are qualitatively capable of explaining the structure and conformation barriers in many molecular systems. The smaller is the value of HOMO–LUMO energy gap, the more probable it is that the compound has inhibition efficiency.

The inhibiting effect of these compounds can be attributed to their parallel adsorption at the metal surface. The parallel adsorption is attributed to the presence of one or more active centers for adsorption. The results seem to suggest that due to the planar geometry of the inhibitor, the molecular adsorption probably occurs in such a way that the metal surface and the molecular plane are parallel to each other, and that, in this conformations the interaction is dominated by donation and back donation between the molecule and the metal surface. The planer geometry is clear in **Fig. 6**. From **Fig.6**, these molecules have approximately planar structure, which can offer the largest contact area between the inhibitor molecules and the steel surface.

The number of transferred electrons (ΔN) was also calculated according to Eq. (11) **[45-46]**

$$\Delta N = (X_{Fe} - X_{inh})/[(2(\eta_{Fe} - \eta_{inh})] \quad (13)$$

where X_{Fe} and X_{inh} denote the absolute electronegativity of iron and the inhibitor molecule, respectively; η_{Fe} and η_{inh} denote the absolute hardness of iron and the inhibitor molecule, respectively. These quantities are related to electron affinity (A) and ionization potential

$$X = (I + A)/2 \quad (14)$$
$$\eta = (I - A)/2$$

I and A are related in turn to EHOMO and ELUMO

$$I = -E_{HOMO} \quad (15)$$
$$A = -E_{LUMO}$$

Values of X and η were calculated by using the values of I and A obtained from quantum chemical calculation. The theoretical values of XFe and ηFe are 7 and 0 eV/mol, respectively **[45**]. The fraction of electrons transferred from inhibitor to the iron molecule (ΔN) was calculated. According to other reports **[45,46]**, value of ΔN showed inhibition effect resulted from electrons donation.

The dipole moment (μ) is an index that can also be used for the prediction of the direction of a corrosion inhibition process [**47]**. Low values of the dipole moment will favor the accumulation of inhibitor molecules on the metallic surface.

Molecular Electrostatic Potential

The molecular electrostatic potential (MEP) can be used to investigate molecular interactions. If polar molecules approach each other, the initial contact arises from long-range electrostatic attractions. These electrostatic interactions can be either attractive or repulsive. An electropositive part of an approaching molecule will seek to dock to an electronegative region; similarly charged parts will repel each other. Due to the charges and dipole moments in a molecule, an electrostatic field is generated in its environment. **[48,49]**.

The electrostatic potential V(r) that is created in the space around a molecule by its nuclei and electrons (treated as static distributions of charge) is a very useful property for analyzing and predicting molecular reactive behavior. It is rigorously defined and can be determined experimentally as well as computationally. The potential has been particularly useful as an indicator of the sites or regions of a molecule to which an approaching electrophile is initially attracted, and it has also been applied successfully to the study of interactions that involve a certain optimum relative orientation of the reactants.

To predict reactive sites for electrophilic and nucleophilic attacks for the title molecule. The negative (red) regions of MEP were related to electrophilic reactivity and the positive (green) regions to nucleophilic reactivity as shown in **Fig. 7.** As can be seen from the figure, there is a possible site on the title compound for electrophilic attack. The negative region is localized on the nitrogen atom , with a maximum value of -0.09 a.u .

However, a maximum positive region is localized on carbon atom of benzyne ring, with a maximum value of 0.03 a.u. This result provides information concerning the region where the compound can interact intermolecularly and bond covalently.

It could be readily observed that nitrogen atoms had higher charge densities. The regions of highest electron density are generally the sites to which electrophiles attacked. Therefore N, was the active center, which had the strongest ability of bonding to the metal surface. On the other hand, HOMO (**Fig. 8**) was mainly distributed on the area containing Nitrogen atom. Thus, the area containing nitrogen atom was probably the primary site of the bonding.

Conclusion

1. All studied 1,2,3-Benzotriazol shown excellent inhibition properties for the corrosion of carbon steel in 1 M HCl solutions, and the inhibition efficiency increases with increasing the concentration of the inhibitors;
2. The inhibitor efficiencies determined by polarization, EIS, and Weight loss methods are in good agreement.
3. The adsorption model obeys the Langmuir adsorption isotherm at 303K, and the negative values of free energy of adsorption indicated that the adsorption of the 1,2,3-Benzotriazol molecule is a spontaneous process.
4. The values of free energy of adsorption suggest that the inhibition behaviour of these 1,2,3-Benzotriazol derivatives involve two types of interaction, chemisorption and physisorption.

References

[1] S. A. Abd El-Maksoud, "Studies on the effect of pyranocoumarin derivatives on the corrosion of iron in 0.5 M HCl," *Corr. Sci.*, **44**, 803–813 (2002).

[2] B. El Mehdi, B. MeTraisnel, F. Benliss, and M. Lagrenee, "Synthesis and comparative study of the inhibitive effect of some new triazole derivatives towards corrosion of carbon steel in hydrochloric acid solution," *Mater. Chem. Phys.*, **77**, 489–196 (2002).

[3] Y. Feng, K. S. Slow, W. K. Teo, and A. K. Hsieh, "The synergistic effects of propargyl alcohol and potassium iodide on the inhibition of carbon steel in 0.5 M sulfuric acid solution," *Corr. Sci.*, **41**, 829–852 (1999).

[4] M. A. Quraishi and J. Rawat, "Corrosion inhibiting action of tetramethyl-dithia-octaaza-cyclotetradeca-hexaene (MTAH) on the corrosion of carbon steel in hot 20% sulfuric acid," *Mater. Chem. Phys.*, **77**, 43–47 (2002).

[5] M. A. Quraishi and D. Jamal, "Dianils as new and effective corrosion inhibitors for carbon steel in acidic solutions," *Mater. Chem. Phys.*, **78**, 608–613 (2003)
[6] E. E. Ebenso, U. J. Ekbe, B. I. Ita, O. E. Offiong, and. O. J. Ibok, "Effect of molecular structure on the efficiency of amides and thiosemicarbazones used for corrosion inhibition of carbon steel in hydrochloric acid," *Mater. Chem. Phys.*, **60**, 79–90 (1999).
[7] M. El Achouri, S. Kertil, H. M. Gouttaya, B. Nciri, et. al., "Corrosion inhibition of iron in 1 M HCl by some gemini surfactants in the series of alkanediyl-□-□-bis-(dimethyl tetradecyl ammonium bromide)," *Progr. Org. Coat.*, **43**, 267–273 (2001).
[8] F. Touhami, A. Aounili, Y. Abed, B. Hammouti, el. al., "Corrosion inhibition of armco iron in 1 M HCl media by new bipyrazolic derivatives," *Corr. Sci.*, **42**, 929–940 (2000).
[9] D. Chebabe, Z. Ait Chikh, N. Hajjaji, A. Srhiri, and F. Zucchi, "Corrosion inhibition of Armco iron in 1 M HCl solution by alkyltriazoles," *Corr. Sci.*, **45**, 309–320 (2003).
[10] G. Morelli, F. Guidi, and G. Grion, "Tryptamine as a green iron corrosion inhibitor in 0.5 M deaerated sulphuric acid," *Corr. Sci.*, **46**, 387–403 (2004).
[11] F. Thouhami, B. Hammouti, A. Aounili, and S. Ketil, A new bipyrazolic compound as corrosion inhibitor of Armco iron in 1 M HCl medium," *Ann. Chim. Sci. Mat.*, **24**, 581–586 (1999).
[12] K. F. Khaled, "The inhibition effect of benzimidazole derivatives on the corrosion of iron in 1 M HCl solutions," *Electrochimica Acta*, **48**, 2493–2503 (2003).
[13] Lj. M. Vracar and D. M. Drazic, "Adsorption and corrosion inhibitive properties of some organic molecules on iron electrode in sulfuric acid," *Corr. Sci.*, **44**, 1669–1680 (2002).
[14] S. Kertit and B. Hammouti, "Corrosion inhibition of iron in 1 M HCl by l-phenyl-5-mercapto-1, 2, 3, 4-tetrazole," *Appl. Surf. Sci.*, **93**, 59–66 (1996).
[15] M. A. Quraishi, F. A. Ansari, and D. Jamal, "Thiourea derivatives as corrosion inhibitors for carbon steel in formic acid," *Mater. Chem. Phys.*, **77**, 687–690 (2002).
[16] A. Chelouani, A. Aouniti, B. Hammouti, N. Benchat, et. al., "Corrosion inhibitors for iron in hydrochloric acid solution by newly synthesized pyridazine derivatives," *Corr. Sci.*, **45**, 1675–1684 (2003).
[17] Wu Yinqiu, Philip R. Herrington, Thermal reactions of fatty acids with diethylene triamine, JAOCS 74 (1997) 1.
[18] R.E. Ford, C.G.L. Furmidge, Studies at phase interfaces: II. The stabilization of water-in-oil emulsions using oil-soluble emulsifiers, J. Colloid Interface Sci. 22 (1966) 331–341.
[19] K.F. Khaled, Electrochim. Acta **48** (17) (2003) 2493.
[20] A.M. A1 Sabagh, Surface and thermodynamic properties ofp-alkylbenzenepolyethoxylated and glyceratedsulfonate derivative surfactants, Colloids and Surfaces A: Physicochem. Eng. Aspects 134 (1998) 313-320
[21] Md. SayemAlam a, AsitBaranMandal, Thermodynamic studies on mixed micellization of amphiphilic drug amitriptyline hydrochloride and nonionic surfactant Triton X-100, Journal of Molecular Liquids 168 (2012) 75–79.
[22] .I.B. Obot, N.O. Obi-Egbedi, Anti-corrosive properties of xanthone on mild steel corrosion in sulphuric acid: Experimental and theoretical investigations, Current Applied Physics 11 (2011) 382-392.
[23] Xianghong L, Shuduan Deng, Hui Fu, Taohong Li, Adsorption and inhibition effect of 6-benzylaminopurine on cold rolled steel in 1.0 M HCl,ElectrochimicaActa 54 (2009) 4089–4098.
[24] Da-Quan Zhang, Qi-RuiCai, Xian-Ming He, Li-XinGao, Gui Soon Kim, Corrosion inhibition and adsorption behavior of methionine on copper in HCl and synergistic effect of zinc ions, Materials Chemistry and Physics 114 (2009) 612–617.
[25] .HulyaKeles, Mustafa Keles, IlyasDehri, Osman Serindag, The inhibitive effect of 6-amino-m-cresol and its Schiff base on the corrosion of mild steel in 0.5 M HCI medium, Materials Chemistry and Physics 112 (2008) 173–179.
[26] .Ramazan Solmaza, EceAltunbas, GülfezaKardas, Adsorption and corrosion inhibition effect of 2-((5-mercapto-1,3,4-thiadiazol-2-ylimino)methyl)phenol Schiff base on mild steel, Materials Chemistry and Physics 125 (2011) 796–801.
[27] R. Solmaz, G. Kardas, B. Yazıcı, M. Erbil, Adsorption and corrosion inhibitive properties of 2-amino-5-mercapto-1,3,4-thiadiazole on mild steel in hydrochloric acid media, Colloids and Surfaces A: Physicochem. Eng. Aspects 312 (2008) 7–17.
[28] .E. McCafferty and N. Hackerman, J. Electrochem. Soc. 119 (1972) 146.
[29] W. J.Lorenz, F. Mansfeld, Corros. Sci. 21(1981)647.
[30] A.A. Aksut, W.J. Lorenz, F. Mansfeld, Corros. Sci. 22 (1982) 611.
[31] B.Gao, X.Zhang, Y Sheng, Mater. Chem. Phys.108(2008) 379.
[32] H. Ashassi-Sorkhabi, M.R. Majidi, K. Seyyedi, Appl. Surf. Sci. 225 (2004) 176.
[33] H. Ashassi-Sorkhabi, N. Ghalebsaz-Jeddi, F. Hashemzadeh, H. Jahani, Electrochim. Acta 51 (2006) 3848.
[34] T. Tsuru, S. Haruyama, B. Gijutsu, J. Jpn. Soc. Corros. Eng. 27 (1978) 573.
[35] F.Bentiss, M. Traisnel, M. Lagrene´e, Corros. Sci. 42 (2000)127.
[36] Bahrami M. J., Hosseini S.M. A. and Pilvar P. (2010) Corros. Sci. **52** (2793)
[37] Fukui K (1975) Theory of orientation and stereo selection. Springer-Verlag, New York
[38] Zhang DQ, Gao LW, Zhou GD (2004) Corros Sci 46:3031
[39] Gao G, Liang C (2007) Electrochim Acta 52:4554
[40] Feng Y, Chen S, Guo Q, Zhang Y, Liu G (2007) J Electroanalytical Chem 602:115
[41] Henriquez-Roman JH, Padilla-Campos L, Paez MA, Zagal JH, Rubio MA, Rangel CM, Costamagna J, Cardenas-Jron G (2005) J Mol Struct (THEOCHEM) 757:1
[42] Ma H, Chen S, Liu Z, Sun Y (2006) J Mol Struct (THEOCHEM) 774:19
[43] Feng Y, Chen S, Zhang H, Li P, Wu L, Guo W (2006) Appl Surf Sci 253:2812
[44] Hasanov R, Sadıkog˘lu M, Bilgic¸ S (2007) Appl Surf Sci ,253:3913
[45] Luque, F. J., Lopez, J. M., & Orozco, M. (2000). Theor. Chem. Accounts, 103, 343.
[46] Okulik, N. & Jubert, A. H. (2005). Internet Electron. J. Mol. Des., 4, 17.
[47] Politzer, P., Laurence, P. R., & Jayasuriya, K. (1985). Environ. Health Perspect. [Special issue], 61, 191.
[48] Scrocco, E., & Tomasi, J. (1973). Topics in Current Chemistry, Springer: Berlin.
[49] Politzer, P., & Truhlar, D. G. (1981). Chemical Applications of Atomic and Molecular Electrostatic Potentials, Plenum: New York.